Two-Dimensional Transient Thermoelastic Problem of a Annular Disc Due to Radiation

Warsha K. Dange[1]

[1]*Department of Mathematics, Shree. Shivaji Arts Commerce And Science College Rajura , India.*

Abstract— The present paper deals with the determination of temperature distribution, displacement components, Goodier's thermoelastic displacement potential, Michell's function and thermal stresses of annular disc occupying the space D : $a \le r \le b,\ -h \le z \le h,$ with boundary conditions of the radiation type. I apply integral transform techniques to find the thermoelastic solution. The results are obtained as series of Bessel functions. Numerical calculations are carried out for annular disc made of aluminium metal and illustrated graphically.

Key words : thermoelastic problem, annular disc, temperature distribution, thermal stress, integral transform

Introduction :

Roy Choudhuri [4] has succeeded in determining the quasi-static thermal stresses in a circular plate subjected to transient temperature along the circumference of circular upper face with lower face at zero temperature and the fixed circular edge thermally insulated. Wankhede [5] has determined the quasi-static thermal stresses in circular plate subjected to arbitrary initial temperature on the upper face with lower face at zero temperature. However, there aren't many investigations on transient state. Deshmukh et al. [3] have determined quasi-static thermal stresses in a thick annular disc. Khobragade et al. [2] have determined thermal deflection of a thin circular plate with radiation . Dange [1] has determined thermal stresses of two –dimensional transient thermoelastic problem of hallow cylinder.

In all aforementioned investigations, they have not however considered any thermoelastic problem with boundary conditions of radiation type, which satisfies the time-dependent heat conduction equation. This paper is concerned with transient thermoelastic problem of a annular disc occupying the space D : $a \le r \le b,\ -h \le z \le h,$ with boundary conditions of the radiation type.

Statement Of The Problem :

Consider the thick annular disc whose axis is coincident with z-axis, defined by $a \le r \le b,$ and $-h \le z \le h,$ where a and b are the internal and external radii respectively and (r, z, t) are cylindrical coordinates. Heat conduction problem and the prescribed boundary conditions of the radiation type are considered with symmetry with respect to the z-axis. Then the temperature $T(r, z, t)$ at any point and thermal stresses of the disc are required to be determined. The equation for heat conduction is $T(r, z, t),$ the temperature, in cylindrical coordinates, is:

$$\kappa\left[\frac{1}{r}\frac{\partial}{\partial r}\left(r\frac{\partial T}{\partial r}\right)+\frac{\partial^2 T}{\partial z^2}\right]=\frac{\partial T}{\partial t} \tag{1}$$

Subject to the initial and boundary conditions

$$M_t(T,1,0,0)=0 \text{ for all } a\le r\le b\ ,\ -h\le z\le h \tag{2}$$

$$M_r(T,1,k_1,a)=0,\ M_r(T,1,k_2,b)=0 \text{ for all } -h\le z\le h\ ,\ t>0 \tag{3}$$

$$M_z(T,1,k_3,h)=o\ \ M_z(T,1,k_4,-h)=\exp(-\omega t)\delta(r-r_0) \text{ for all } a\le r\le b\ ,\ t>0 \tag{4}$$

Where $\exp(-\omega t)\delta(r-r_0)$ is the additional sectional heat available on its surface at $z=-h$; κ is the thermal diffusivity of the material of the disc (which is assumed to be constant); λ being the thermal conductivity of the material. The most general expression for these conditions can be given by

$$M_{\vartheta}(f,\bar{k},\bar{\bar{k}},\$)=(\bar{k}\ f+\bar{\bar{k}}\ \hat{f})_{\vartheta=\$}$$

with prime (^) denotes as differentiation with respect to ϑ; $\delta(r-r_0)$ is the Dirac Delta function having $a\le r_0\le b$; $\omega>0$ is a constants; $\bar{k}$ and $\bar{\bar{k}}$ are radiation coefficients of the disc, respectively.

The Navier's equations without the body forces for axisymmetric two-dimensional thermoelastic problem can be expressed as

$$\left.\begin{aligned}\nabla^2 u_r-\frac{u_r}{r^2}+\frac{1}{1-2\upsilon}\frac{\partial e}{\partial r}-\frac{2(1+\upsilon)}{1-2\upsilon}\alpha_t\frac{\partial T}{\partial r}=0\\ \nabla^2 u_z-\frac{1}{1-2\upsilon}\frac{\partial e}{\partial z}-\frac{2(1+\upsilon)}{1-2\upsilon}\alpha_t\frac{\partial T}{\partial z}=0\end{aligned}\right\} \tag{5}$$

where u_r and u_z are the displacement components in the radial and axial directions respectively and the dilatation e as

$$e=\frac{\partial u_r}{\partial r}+\frac{u_r}{r}+\frac{\partial u_z}{\partial z}$$

The displacement function in the cylindrical coordinate system are represented by the Goodier's thermoelastic displacement potential ϕ and Michell's function M as

$$u_r=\frac{\partial\phi}{\partial r}-\frac{\partial^2 M}{\partial r\partial z}, \tag{6}$$

$$u_z=\frac{\partial\phi}{\partial z}+2(1-\upsilon)\nabla^2 M-\frac{\partial^2 M}{\partial^2 z} \tag{7}$$

in which Goodier's thermoelastic potential must satisfy the equation

$$\nabla^2\phi=\left(\frac{1+\upsilon}{1-\upsilon}\right)\alpha_t T \tag{8}$$

and the Michell's function M must satisfy the equation

$$\nabla^2(\nabla^2 M) = 0 \tag{9}$$

Where

$$\nabla^2 = \frac{1}{r}\frac{\partial}{\partial r}\left(r\frac{\partial}{\partial r}\right) + \frac{\partial^2}{\partial z^2}$$

The component of the stresses are represented by the use of the potential ϕ and Michell's function M as

$$\sigma_{rr} = 2G\left\{\left(\frac{\partial^2\phi}{\partial r^2} - \nabla^2\phi\right) + \frac{\partial}{\partial z}\left(\upsilon\nabla^2 M - \frac{\partial^2 M}{\partial r^2}\right)\right\}, \tag{10}$$

$$\sigma_{\theta\theta} = 2G\left\{\left(\frac{1}{r}\frac{\partial\phi}{\partial r} - \nabla^2\phi\right) + \frac{\partial}{\partial z}\left(\upsilon\nabla^2 M - \frac{1}{r}\frac{\partial M}{\partial r}\right)\right\}, \tag{11}$$

$$\sigma_{zz} = 2G\left\{\left(\frac{\partial^2\phi}{\partial r^2} - \nabla^2\phi\right) + \frac{\partial}{\partial z}\left((2-\upsilon)\nabla^2 M - \frac{\partial^2 M}{\partial z^2}\right)\right\}, \tag{12}$$

and

$$\sigma_{rz} = 2G\left\{\frac{\partial^2\phi}{\partial r\partial z} + \frac{\partial}{\partial r}\left((1-\upsilon)\nabla^2 M - \frac{\partial^2 M}{\partial z^2}\right)\right\} \tag{13}$$

where G and υ are the shear modulus and Poisson's ratio respectively.

The equations (1) to (13) constitute the mathematical formulation of the problem under consideration.

Solution of the problem:

Results Required:

In order to solve fundamental differential equation (1) under the boundary condition (3), first introduce the integral transform of order n over the variable r. Let n be the parameter of the transform, then the integral transform and its inversion theorem are written as

$$\bar{g}(n) = \int_a^b r\, g(r)\, S_p(k_1, k_2, \mu_n r)\, dr, \quad g(r) = \sum_{n=1}^{\infty} (\bar{g}_p(n)/C_n)\, S_p(k_1, k_2, \mu_n r) \tag{14}$$

where $\bar{g}_p(n)$ is the transform of $g(r)$ with respect to nucleus $S_p(k_1, k_2, \mu_n r)$.

The Eigen values μ_n are the positive roots of the characteristic equation

$$J_0(k_1, \mu a)\, Y_0(k_2, \mu b) - J_0(k_2, \mu b)\, Y_0(k_1, \mu a) = 0$$

The kernel function $S_0(k_1, k_2, \mu_n r)$ can be defined as

$$S_0(k_1, k_2, \mu_n r) = J_0(\mu_n r)[Y_0(k_1, \mu_n a) + Y_0(k_2, \mu_n b)] - Y_0(\mu_n r)[J_0(k_1, \mu_n a) + J_0(k_2, \mu_n b)]$$

with

$$\left.\begin{aligned} J_0(k_i, \mu r) &= J_0(\mu r) + k_i\, \mu J_0'(\mu r) \\ Y_0(k_i, \mu r) &= Y_0(\mu r) + k_i\, \mu Y_0'(\mu r) \end{aligned}\right\} \quad \text{for} \quad i = 1, 2$$

and

$$C_n = \int_a^b r[S_0(k_1, k_2, \mu_n b)]^2 dr$$

in which $J_0(\mu r)$ and $Y_0(\mu r)$ are Bessel functions of first and second kind of order $p = 0$ respectively.

Again introduce another integral transform that responds to the boundary conditions of type

$$\overline{f}(m) = \int_{-h}^{h} f(z) P_m(z)\, dz, \quad f(z) = \sum_{m=1}^{\infty} \frac{\overline{f}(m)}{\lambda_m} P_m(z) \tag{15}$$

where $\overline{f}(m)$ is the transformed function of $f(z)$ and m is the transform parameter. The nucleus is given by the orthogonal functions in the interval $-h \le z \le h$ as

$$P_m(z) = Q_m \cos(a_m z) - W_m \sin(a_m z)$$

where

$$Q_m = a_m (k_3 + k_4) \cos(a_m h),$$

$$W_m = 2\cos(a_m h) + (k_3 - k_4) a_m \sin(a_m h),$$

$$\lambda_m = \int_{-h}^{h} P_m^2(z)\, dz = h[Q_m^2 + W_m^2] + \frac{\sin(2a_m h)}{2a_m}[Q_m^2 - W_m^2]$$

The eigen values a_m are the positive roots of the characteristic equation

$$\begin{aligned} &[k_3\, a\cos(ah) + \sin(ah)]\,[\cos(ah) + k_4\, a\sin(ah)] \\ &= [k_4\, a\cos(ah) - \sin(ah)]\,[\cos(ah) - k_3\, a\sin(ah)] \end{aligned}$$

Determination of Temperature Function $T(r, z, t)$:

Applying the transform defined in equation (14) to the equations (1), (2) and (4), and using equation (3) to reduce the differential equation in Marchi- Zgrablich transform domain and then applying Marchi- Fasulo transform defined in equation (15) and making use of respective inversion as in (15) and (14) over the heat conduction equation one obtains the expression for temperature distribution function as

$$T(r, z, t) = \sum_{n=1}^{\infty} \frac{1}{C_n} \left\{ \sum_{m=1}^{\infty} \frac{\Omega_{n,m}}{\lambda_m(\kappa(\mu_n^2 + a_m^2) - \omega)} [\exp(-\omega t) - \exp(-\kappa(\mu_n^2 + a_m^2)t)]\, P_m(z) \right\} \times S_0(k_1, k_2, \mu_n r) \tag{16}$$

Where

$$\Omega_{n,m} = -k\left[\frac{P_m(-h)}{k_4}\right] r_0\, S_0(k_1, k_2, \mu_n r_0)$$

Determination Of Thermoelastic Displacement Potential $\phi(r,z,t)$:

Substituting the value of $T(r,z,t)$ from equation (16) to equation (8) one obtains the thermoelastic displacement function $\phi(r,z,t)$ as.

$$\phi(r,z,t)=-\left(\frac{1+\upsilon}{1-\upsilon}\right)\alpha_t\sum_{n=1}^{\infty}\frac{1}{C_n}\left\{\sum_{m=1}^{\infty}\frac{\Omega_{n,m}}{\lambda_m(\kappa(\mu_n^2+a_m^2)-\omega)(\mu_n^2+a_m^2)}[\exp(-\omega t)-\exp(-\kappa(\mu_n^2+a_m^2)\,t)]P_m(z)\right\}\times S_0(k_1,k_2,\mu_n r) \tag{17}$$

Determination Of Michell's Function $M(r,z,t)$:

Using equation (9) one obtains the Michell's function $M(r,z,t)$ as

$$M(r,z,t)=-\left(\frac{1+\upsilon}{1-\upsilon}\right)\alpha_t\sum_{n=1}^{\infty}\frac{1}{C_n}\left\{\sum_{m=1}^{\infty}\frac{\Omega_{n,m}}{\lambda_m(\kappa(\mu_n^2+a_m^2)-\omega)(\mu_n^2+a_m^2)}[\exp(-\omega t)-\exp(-\kappa(\mu_n^2+a_m^2)\,t)]\right\}$$
$$\times\left[\sinh(\mu_n z)+z\cosh(\mu_n z)\right]\times S_0(k_1,k_2,\mu_n r) \tag{18}$$

Determination Of *Displacement* Components u_r, u_z:

Now, in order to obtain the displacement components, substitute the values of thermoelastic displacement potential ϕ and Michell's function M in equations (6) and (7), one obtains

$$u_r=-\left(\frac{1+\upsilon}{1-\upsilon}\right)\alpha_t\sum_{n=1}^{\infty}\frac{1}{C_n}\left\{\sum_{m=1}^{\infty}\frac{\Omega_{n,m}}{\lambda_m(\kappa(\mu_n^2+a_m^2)-\omega)(\mu_n^2+a_m^2)}[\exp(-\omega t)-\exp(-\kappa(\mu_n^2+a_m^2)\,t)]\right\}$$
$$\times\left[P_m(z)-(\mu_n+1)\cosh(\mu_n z)-\mu_n z\sinh(\mu_n z)\right]\mu_n\ S_0'(k_1,k_2,\mu_n r) \tag{19}$$

$$u_z=-\left(\frac{1+\upsilon}{1-\upsilon}\right)\alpha_t\sum_{n=1}^{\infty}\frac{1}{C_n}\left\{\sum_{m=1}^{\infty}\frac{\Omega_{n,m}}{\lambda_m(\kappa(\mu_n^2+a_m^2)-\omega)(\mu_n^2+a_m^2)}[\exp(-\omega t)-\exp(-\kappa(\mu_n^2+a_m^2)\,t)]\right\}$$
$$\times[-a_m(Q_m\sin(a_m z)-W_m\cos(a_m z))+2(1-2\upsilon)\mu_n\sinh(\mu_n z)$$
$$-\mu_n^2(\sinh(\mu_n z)+z\cosh(\mu_n z))]\times S_0(k_1,k_2,\mu_n r) \tag{20}$$

Thus making use of the two displacement components the dilation is established as

$$e=\left(\frac{1+\upsilon}{1-\upsilon}\right)\alpha_t\sum_{n=1}^{\infty}\frac{1}{C_n}\left\{\sum_{m=1}^{\infty}\frac{\Omega_{n,m}}{\lambda_m(\kappa(\mu_n^2+a_m^2)-\omega)(\mu_n^2+a_m^2)}[\exp(-\omega t)-\exp(-\kappa(\mu_n^2+a_m^2)\,t)]\right\}$$
$$\left[(\mu_n^2+a_m^2)P_m(z)-2(1-2\upsilon)\mu_n^2\cosh(\mu_n z)\right]S_0(k_1,k_2,\mu_n r) \tag{21}$$

Determination Of Stress Components σ_{rr}, $\sigma_{\theta\theta}$, σ_{zz} And σ_{rz} :

The stress components can be evaluated by substituting the values of thermoelastic displacement potential ϕ from equation (17) and Michell's function M from equation (18) in equations (10), (11), (12) and (13), one obtains

$$\sigma_{rr} = -2G\left(\frac{1+\upsilon}{1-\upsilon}\right)\alpha_t \sum_{n=1}^{\infty}\frac{1}{C_n}\left\{\sum_{m=1}^{\infty}\frac{\Omega_{n,m}}{\lambda_m(\kappa(\mu_n^2+a_m^2)-\omega)(\mu_n^2+a_m^2)}[\exp(-\omega t)-\exp(-\kappa(\mu_n^2+a_m^2)\,t)]\right\}$$
$$\times\left\{\left[(\mu_n^2+a_m^2)^{-1}\mu_n^2[P_m(z)-(\mu_n+1)\cosh(\mu_n z)-z\,\mu_n\sinh(\mu_n z)]\right]S_0''(k_1,k_2,\mu_n r)\right.$$
$$\left.-\left[P_m(z)-2(\mu_n^2+a_m^2)^{-1}\upsilon\mu_n^2\cosh(\mu_n z)\right]\right\}S_0(k_1,k_2,\mu_n r)\Big] \qquad (22)$$

$$\sigma_{\theta\theta} = -2G\left(\frac{1+\upsilon}{1-\upsilon}\right)\alpha_t \sum_{n=1}^{\infty}\frac{1}{C_n}\left\{\sum_{m=1}^{\infty}\frac{\Omega_{n,m}}{\lambda_m(\kappa(\mu_n^2+a_m^2)-\omega)(\mu_n^2+a_m^2)}[\exp(-\omega t)-\exp(-\kappa(\mu_n^2+a_m^2)\,t)]\right\}$$
$$\left[\mu_n(\mu_n^2+a_m^2)^{-1}r^{-1}[P_m(z)-(\mu_n+1)\cosh(\mu_n z)-z\,\mu_n\sinh(\mu_n z)]\right]S_0'(k_1,k_2,\mu_n r)$$
$$-\left[P_m(z)+2(\mu_n^2+a_m^2)^{-1}\upsilon\mu_n^2\cosh(\mu_n z)\right]S_0(k_1,k_2,\mu_n r) \qquad (23)$$

$$\sigma_{zz} = -2G\left(\frac{1+\upsilon}{1-\upsilon}\right)\alpha_t \sum_{n=1}^{\infty}\frac{1}{C_n}\left\{\sum_{m=1}^{\infty}\frac{\Omega_{n,m}}{\lambda_m(\kappa(\mu_n^2+a_m^2)-\omega)(\mu_n^2+a_m^2)}[\exp(-\omega t)-\exp(-\kappa(\mu_n^2+a_m^2)\,t)]\right\}$$
$$\left[P_m(z)\mu_n^2(\mu_n^2+a_m^2)^{-1}S_0''(k_1,k_2,\mu_n r)-\left[P_m(z)-(\mu_n^2+a_m^2)^{-1}\right.\right.\left[2(2-\upsilon)\mu_n^2\cosh(\mu_n z)-\right.$$
$$\left.\left.\mu_n^2\sinh(\mu_n z)+2\mu_n\sinh(\mu_n z)+z\mu_n^2\cosh(\mu_n z)\right]S_0(k_1,k_2,\mu_n r)\right. \qquad (24)$$

$$\sigma_{rz} = -2G\left(\frac{1+\upsilon}{1-\upsilon}\right)\alpha_t \sum_{n=1}^{\infty}\frac{1}{C_n}\left\{\sum_{m=1}^{\infty}\frac{\Omega_{n,m}}{\lambda_m(\kappa(\mu_n^2+a_m^2)-\omega)(\mu_n^2+a_m^2)}[\exp(-\omega t)-\exp(-\kappa(\mu_n^2+a_m^2)\,t)]\right\}$$
$$\times\{-a_m\mu_n[Q_m\sin(a_m z)+W_m\cos(a_m z)]-2\upsilon\mu_n{}^2\sinh(\mu_n z)$$
$$-\mu_n^3[\sinh(\mu_n z)+z\cosh(\mu_n z)]\}S_0'(k_1,k_2,\mu_n r) \qquad (25)$$

Numerical Results, Discussion and Remarks:

To interpret the numerical computations, consider material properties of Aluminium metal. The foregoing analysis performed by setting the radiation coefficients constants, $k_1 = k_2 = 1$, Thermal diffusivity κ=0.86 cm^2/sec ,Poisson ratio, υ= 0.281, Thermal expansion coefficient, α_t (cm/cm-^{0}C) =25.5 $\times$ 10^{-6} , Shear Modulus , G[N/cm^2] = 2.7 $\times$ 10^6 , Inner radius, a (cm)=1, Outer radius, b (cm) = 2, *Height h* (cm) = 0.5. The other parameters considered are r_0 (cm)= 1.5, and ω = 1.

Numerical results from (16)-(25) have been illustrated graphically (From figure 1-9)

Figure 1 represents graph of T versus **r** for different values of **t** . It is observed that T increases from $r = 1$ to $r = 1.2$. Also it observed that T develops tensile stresses from $r = 1.2$ to $r = 1.6$. From $r = 1.6$ to $r = 1.8$

$T(r,z,t)$ is approximately zero and from $r=1.8$ to $r=2$ it is again goes on increasing in the circular region of the annular disc for different values of t.

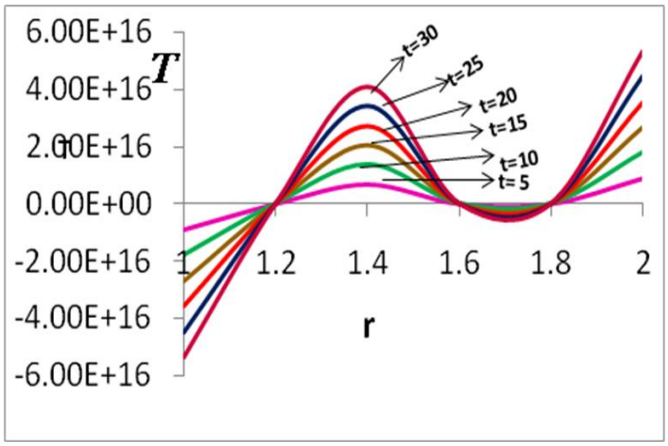

Fig 1: Graph of T versus r for different values of t

Figure 2 represents graph of $\phi(r,z,t)$ versus **r** for different values of **t** . It is observed that $\phi(r,z,t)$ goes on increasing from $r=1$ to $r=2$ in the circular region of the annular disc for different values of t.

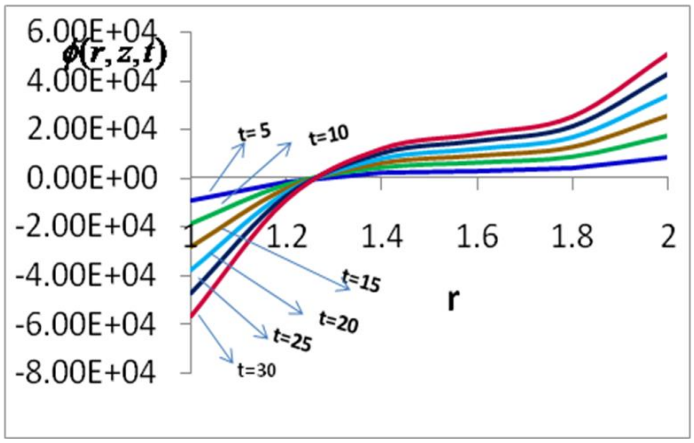

Fig 2: Graph of $\phi(r,z,t)$ versus r for different values of t

Figure 3: represents graph of $M(r,z,t)$ versus **r** for different values of **t** . It is observed that $M(r,z,t)$ increases from $r=1$ to $r=1.2$ and from $r=1.8$ to $r=2$ it is also observed that M develops compressive stresses from $r=1.2$ to $r=1.6$. $M(r,z,t)$ is approximately zero from $r=1.6$ to $r=1.8$ in the circular region of the annular disc for different values of t.

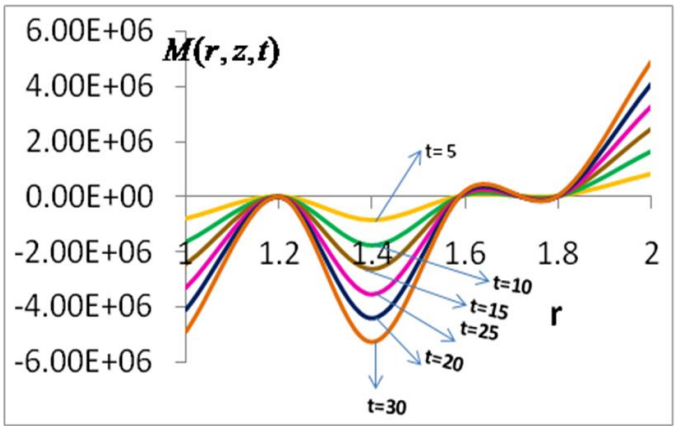

Fig 3: Graph of $M(r,z,t)$ versus r for different values of t

Figure 4: represents graph of u_r versus **r** for different values of **t** . It is observed that u_r goes on decreasing from $r=1$ to $r=1.2$ and from $r=1.8$ to $r=2$ it is also observed that u_r develops compressive stresses from $r=1.2$ to $r=1.6$. u_r is approximately zero from $r=1.6$ to $r=1.8$ in the circular region of the annular disc for different values of t.

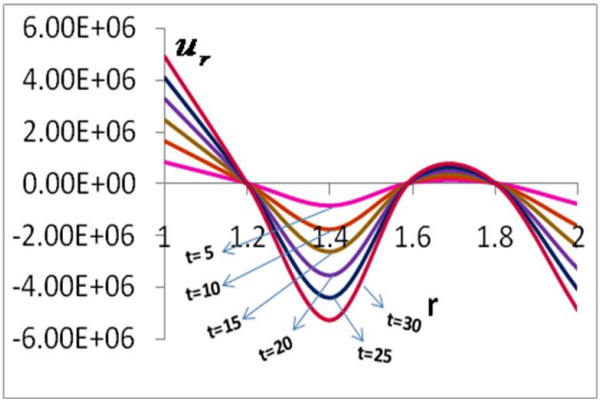

Fig 4: Graph of u_r versus r for different values of t

Figure 5: represents graph of u_z versus **r** for different values of **t** . It is observed that u_z goes on decreasing from $r=1$ to $r=1.2$ and from $r=1.8$ to $r=2$ it is also observed that u_z develops tensile stresses from $r=1.4$ to $r=1.8$ in the circular region of the annular disc for different values of t.

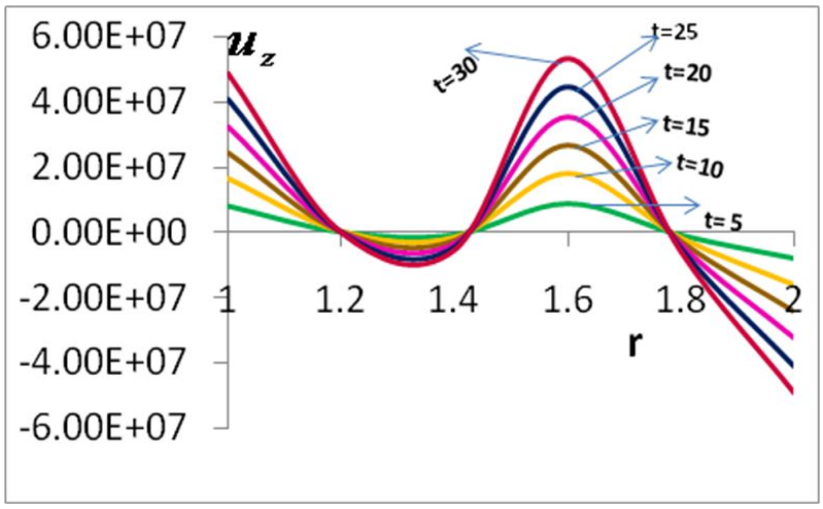

Fig 5: Graph of u_z versus r for different values of t

Figure 6: represents graph of σ_{rr} versus **r** for different values of **t** . It is observed that σ_{rr} develops compressive stresses from $r = 1.2$ to $r = 1.6$. it is also observed that σ_{rr} is approximately zero from $r = 1$ to $r = 1.2$ and from $r = 1.6$ to $r = 2$ in the circular region of the annular disc for different values of t. .

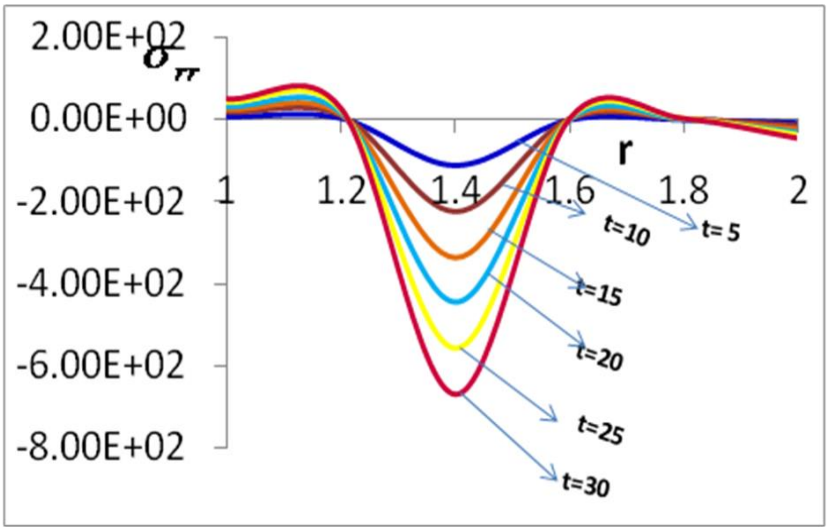

Fig 6: Graph of σ_{rr} versus r for different values of t

Figure 7: represents graph of $\sigma_{\theta\theta}$ versus **r** for different values of **t** . It is observed that $\sigma_{\theta\theta}$ develops tensile stresses from $r = 1.4$ to $r = 1.8$. it is also observed that $\sigma_{\theta\theta}$ is approximately zero from $r = 1$ to $r = 1.4$ and $\sigma_{\theta\theta}$ goes on decreasing from $r = 1.8$ to $r = 2$ in the circular region of the annular disc for different values of t. .

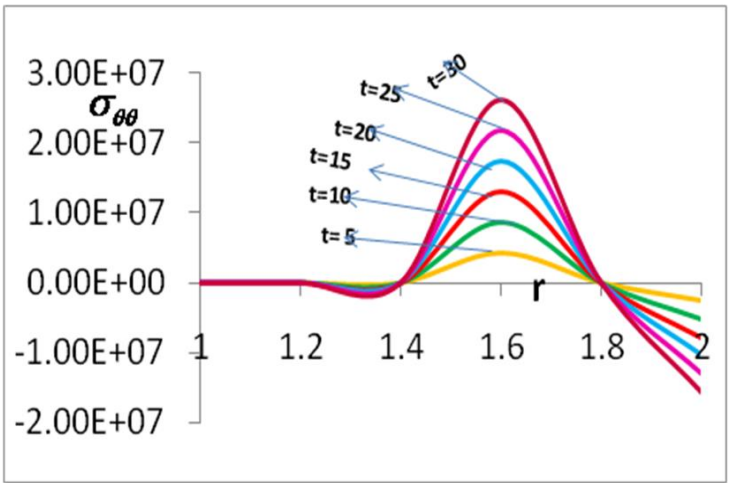

Fig 7: Graph of $\sigma_{\theta\theta}$ versus r for different values of t

Figure 8: represents graph of σ_{rz} versus **r** for different values of **t** . It is observed that σ_{rz} develops tensile stresses from $r = 1.2$ to $r = 1.6$. it is also observed that σ_{rz} is approximately zero from $r = 1$ to $r = 1.2$ and σ_{rz} goes on decreasing from $r = 1.6$ to $r = 2$ in the circular region of the annular disc for different values of t.

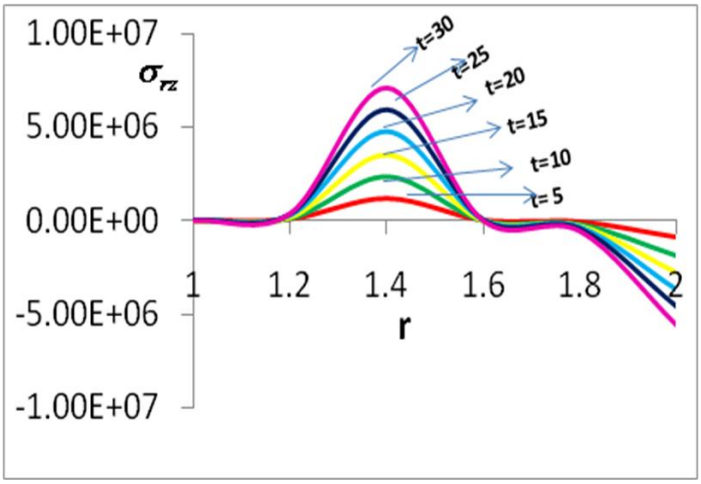

Fig 8: Graph of σ_{rz} versus r for different values of t

Figure 9: represents graph of σ_{zz} versus **r** for different values of **t** . It is observed that σ_{zz} develops tensile stresses from $r = 1$ to $r = 1.3$ and compressive stresses from $r = 1.3$ to $r = 1.6$. it is also observed that σ_{zz} is approximately zero from $r = 1.6$ to $r = 1.8$ and σ_{zz} goes on decreasing from $r = 1.8$ to $r = 2$ in the circular region of the annular disc for different values of t.

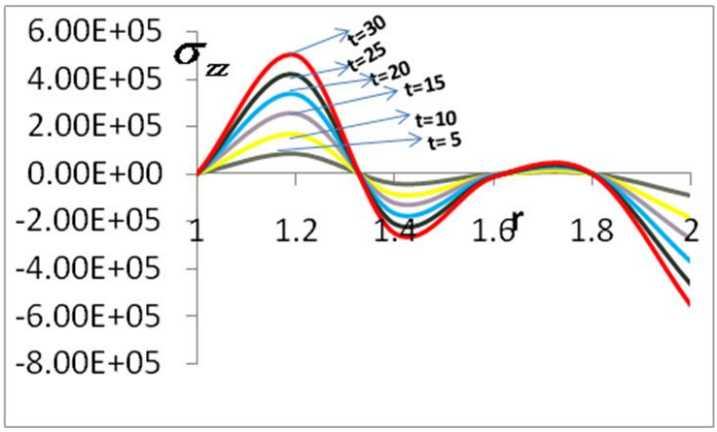

Fig 9: Graph of σ_{zz} versus r for different values of t

Conclusion :

In this study, I treated the two-dimensional thermoelastic problem of a annular disc with additional sectional heat, $\exp(-\omega t)\delta(r-r_0)$ available on its surfaces z = -h.. Under given conditions temperature distribution, displacement components, Goodiers thermoelastic displacement potential, Michell's function and thermal stresses have been determined with the help of Marchi- Zgrablich transform, Marchi- Fasulo transform techniques. Any particular case can be derived by assigning suitable values to the parameters and functions in the expressions .I may conclude that the system of equations proposed in this study can be adopted to design of useful structures or machines in engineering application in the determination of thermoelastic behaviour and illustrated graphically.

Acknowledgement :

The author is thankful to **prof. Anand Raipure** for kind help in the preparation of this paper.

References :

[1] **Dange W.K.,** Thermal Stresses Of Two –Dimensional Transient Thermoelastic Problem Of Hallow Cylinder, International Journal of Engineering and Innovative Technology (IJEIT), Vol. 4,issue 6, 106-109,December 2014

[2] **Khobragade N.W.** ,Hamana Parveen,Lama N. thermal deflection of a thin circular plate with radiation , African journal of mathematics and computer science research , Vol. 5 (4) (2012), 66-70.

[3] **Kulkarni, V. S. , K. C. Deshmukh, K. C. ,** Quasi-static transient thermal stresses in a thick annular disc, Sādhanā, 32 (2007) 561–575.

[4] **Roy Choudhary, S. K.** A note on quasi-static thermal deflection of a thin clamped circular plate due to ramp-type heating of a concentric circular region of the upper face, J. of the Franklin Institute, 206 (1973), 213-219.

[5] **Wankhede, P. C.** On the quasi-static thermal stresses in a circular plate, Indian J. Pure Appl. Math., Vol. 13 (8) (1982), 1273-1277.